Photoelectrocatalysis

International Edition: DOI: 10.1002/anie.201509567
German Edition: DOI: 10.1002/ange.201509567

Curing $BiVO_4$ Photoanodes with Ultraviolet Light Enhances Photoelectrocatalysis

*Tengfei Li, Jingfu He, Bruno Peña, and Curtis P. Berlinguette**

Abstract: *Exposure of $BiVO_4$ photoanodes to ultraviolet (UV) radiation for extended time periods (e.g., 20 h) produces a morphological change and concomitant improvement in photo-electrocatalytic (PEC) efficiency for driving water splitting directly by sunlight. The ~230 mV cathodic shift in onset potential and doubling of the photocurrent at 1.23 V vs. RHE after UV curing are comparable to the effects engendered by the presence of a secondary catalyst layer. PEC measurements and absorption spectra indicate that the cathodic shift after UV curing corresponds to a suppression of charge recombination and a greater photovoltage generation caused by the shift of the flat-band potential, and not an improvement in electrocatalytic activity or light absorption. Spectroscopic surface analysis suggests that surface defect sites, which are eliminated by UV curing, for the differences in observed charge recombination.*

The solar-driven PEC oxidation of water offers the means to store sunlight as hydrogen and oxygen fuels.[1–3] The efficient, direct conversion of photons to these fuels requires a semiconducting material that is competent in both absorbing sufficient amounts of sunlight and mediating the catalytic oxidation of water, potentially augmented by an electrocatalyst layer. Among the materials that have been tested in this context, $BiVO_4$ stands out as one of the best photoelectrocatalysts due to an onset of absorption at 520 nm and band edges appropriately positioned to accommodate the oxygen evolution reaction (OER).[4] The OER onset potential for the $BiVO_4$ photoanode is high, however, thereby requiring nanostructuring of material[5,6] or an additional metal oxide layer (e.g., CoO_x, NiO_x, and FeO_x) to help mediate the multielectron reaction more effectively.[1–3,5,7–9] These secondary metal oxide coatings serve to improve photoelectrocatalysis by either suppressing charge recombination within the photoanode[4–7,10,11] and/or mediating the OER reaction more effectively.[8,12] The mechanism of action notwithstanding, these composite systems will inherently suffer from some efficiency losses due to the additional interface and a masking of the photoactive layer to incident sunlight,[13] thus providing the impetus to discover a photoelectrocatalyst that does not require an additional electrocatalyst coating.

[*] T. Li, J. He, B. Peña, Dr. C. P. Berlinguette
Departments of Chemistry and Chemical & Biological Engineering, The University of British Columbia
2036 Main Mall, Vancouver, BC V6T1Z1 (Canada)
E-mail: cberling@chem.ubc.ca

Supporting information for this article is available on the WWW under http://dx.doi.org/10.1002/anie.201509567.

Pursuant to our goal of developing new oxide materials to access new metal oxide films for energy conversion schemes,[14] we set out to understand how the OER PEC performance of $BiVO_4$ photoanodes is affected by extended exposure to UV radiation. We show herein the unexpected observation that exposure of $BiVO_4$ photoanodes to sustained UV radiation yields a change in electrode morphology that yields a markedly cathodic potential shift of ~400 mV at 1 mA cm^{-2}. Notably, this photolysis procedure is found to enhance the photocurrent of $BiVO_4$ to the same extent as a Co-Pi cocatalyst,[7,8] and provides a fundamentally different yet simple approach for achieving high performance photoanodes compared to previously tested methods. This demonstration of enhanced performance during extended illumination is aligned with the need to develop solar energy conversion technologies that display temporal stability.

The $BiVO_4$ photoanodes under investigation were synthesized in accordance with a protocol developed by Gamelin and co-workers,[7] where appropriate stoichiometric amounts of bismuth nitrate hexahydrate, vanadyl acetylacetonate and tungsten hexachloride dissolved in a solution of acetic acid and acetylacetone were spin-cast onto a conducting layer of fluorine-doped tin oxide (FTO) prior to an annealing step at 500 °C. The resultant films were then exposed to UV radiation (λ_{max} ~185 and 254 nm, ~10 mW cm^{-2}) in air for up to 20 hours.

Scanning electron microscopy (SEM) images of the $BiVO_4$ films not subjected to UV curing (Figure 1a) reveal morphological features consistent with previous descriptions of $BiVO_4$.[7] Images of the films after photolysis reveal a change in features that suggests fusion of the crystalline domains towards a less textured surface (Figure 1b). Atomic force microscopy (AFM) images of $BiVO_4$ also indicate a lower roughness factor after irradiation (Figure S1 in the Supporting Information). These macroscopic modifications during UV photolysis did not render any changes in atomic structure that were detectable by X-ray diffraction (XRD) techniques, as the photoactive monoclinic phase of $BiVO_4$ was measured before and after curing (Figure 1c). Moreover, absorption spectra recorded on the photoanodes before and after photolysis were superimposable (Figure 1d), thus ruling out differences in film absorptivities being responsible for any changes in PEC performance after photolysis of $BiVO_4$.

The PEC current densities of the $BiVO_4$ photoanodes cured by UV radiation for 0 (control), 5 and 20 h in air were then measured, in the dark and under AM1.5 front-side illumination, in a three electrode cell containing a 0.1 M potassium phosphate solution buffered to pH 7 (KPi) (Figure 2). The films that were not exposed to UV radiation displayed an onset potential of 0.65 V vs. RHE and a current

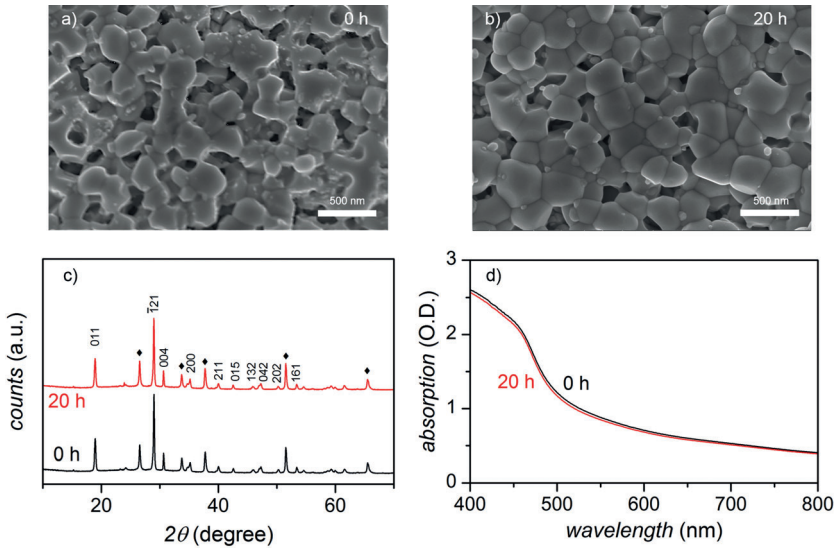

Figure 1. a,b) SEM images, c) powder XRD diffractograms, and d) UV-vis absorption spectra recorded on $BiVO_4$ films coated on FTO glass before and after exposure to 20 h of UV curing. Diffraction signals attributed to FTO are indicated by black diamonds in (c).

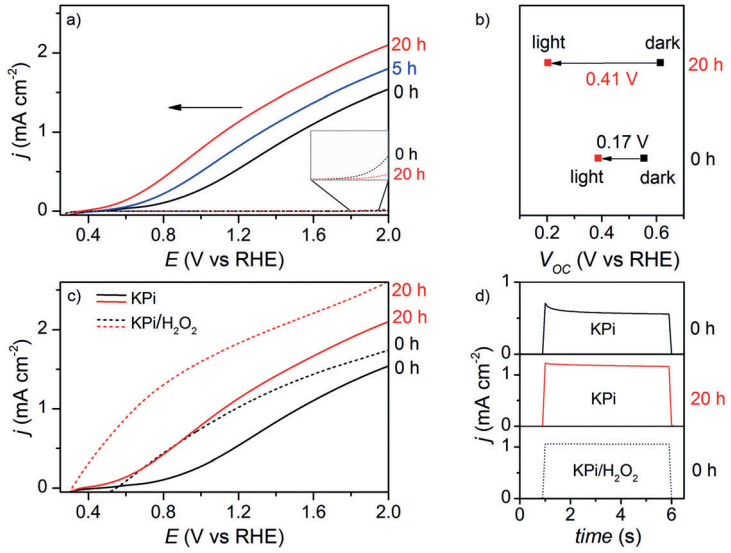

Figure 2. a) Dark current (dashed) and photocurrent (solid; AM1.5 front-side illumination) densities of $BiVO_4$ photoanodes after being subjected to 0 (black), 5 (blue), and 20 (red) hours of UV curing. Data was recorded in a three-electrode cell in KPi buffered solutions (pH 7). b) Open-circuit potentials (V_{OC}), measured in the dark (black) and under AM1.5 illumination (red), of $BiVO_4$ photoanodes before and after 20 h of UV curing. The values indicated correspond to the photovoltages generated by $BiVO_4$, calculated by the difference of V_{OC} between dark and illumination conditions. c) Photocurrent densities of $BiVO_4$ photoanodes, before and after exposure to 20 h of UV curing, in KPi buffered solutions (solid) and after the addition of 0.1 M H_2O_2 (dashed). d) Photocurrent transients measured at 1.23 V vs. RHE of $BiVO_4$ before (black, solid) and after (red, solid) UV curing in KPi. Data for the sample not exposed to UV curing measured in a KPi solution containing H_2O_2 is also shown (black, dashed).

density of 1.0 mA cm^{-2} at 1.52 V vs. RHE. While this electrocatalytic response is commensurate with previously reported $BiVO_4$ films, progressively larger cathodic shifts in onset potentials were measured as the films were exposed to increasing durations of UV curing: The potential required to reach a photocurrent of 1 mA cm^{-2} was reduced to 1.12 V vs. RHE after 20 h of UV curing. This ~400 mV reduction in overpotential is striking in that it is comparable to the effects of metal oxide co-catalysts deposited on $BiVO_4$ (e.g., 440 mV for Co-Pi on $BiVO_4$).[7] The photocurrent densities progressively increase with UV radiation exposure times up to 20 h, with nominal differences over the next 10 h of photolysis (Figure S2). Notably, this enhancement of photocurrent is stable after the cured $BiVO_4$ samples are kept in air and open circuit conditions in KPi solutions (Figure S3 a).

The dark currents of the water oxidation reaction are suppressed after UV curing (Figure 2 a inset and Figure S4 d). This observation implicates a lower number of electrochemically active sites, and is consistent with the lower texture of the photolyzed surfaces (Figure 1). The charging currents are also suppressed after photolysis (Figure S4), consistent with the lower specific surface area indicated by SEM and AFM. On this basis, we rule out the enhancement of photocurrent densities of the cured films being a result of a higher concentration of active sites or a larger specific surface area. The measured photovoltages increase from 0.17 V to 0.41 V after 20 h of UV curing (Figure 2 b), and the photovoltages measured in the presence of H_2O_2, which is capable of proceeding through more facile oxidative chemistry than water, also displayed a ~230 mV cathodic shift in onset potential (Figure 2 c). These collective data indicate that the cathodic shift is due to a larger photovoltage emanating from a shift in flat-band potential upon UV curing, and not electrocatalytic efficacy.[15]

Recombination at the $BiVO_4$ surface was interrogated by measuring the photocurrent transients of $BiVO_4$ photoanodes at 1.23 V vs. RHE (Figure 2 d). Temporal measurements in KPi solutions show a sharp spike in photocurrent, consistent with an accumulation of photo-generated holes at the photoanode/electrolyte interface followed by a slow decay induced from charge recombination.[7] The spikes in current are suppressed in the presence of H_2O_2 due to the lower activation barrier associated with mediating the reaction. This behaviour is different after UV curing, where the photocurrent density in KPi of ~1.2 mA cm^{-2} is twice that measured for the films not exposed to UV light (Figure 2 d); these photocurrents were maintained for at least two hours (Figure S3 b). Moreover, the photocurrent transient profile reveals a significant diminution in current spikes that point to

a reduction in surface recombination processes being responsible for the enhanced PEC activity.

Electrochemical impedance spectroscopy (EIS) was measured on the $BiVO_4$ before and after 20 h of UV curing to better characterize the surface chemistry. Nyquist plots recorded at potentials of 0.5, 0.7 and 0.9 V vs. RHE (Figure 3a; plots recorded under the full potential range are shown in Figure S5) reveal two semicircles at lower potentials, where the second is diminished at higher potentials. These features have been modeled to an equivalent circuit model (Figure 3a inset),[16] where the first semicircle is ascribed to bulk processes and the second to surface processes. The capacitance of the bulk solid, C_{bulk}, follows the regulation of depletion layer capacitance[17] while the second capacitance value, C_{ss}, progressively increases over the 0.5–1.1 V range (Figure S6). This behavior apparently corresponds to the features of surface states.[17,18] As shown in Figure 3b, the substantial increase in photocurrent does not commence until the resistance associated with the surface states is reduced to an extent. This correlation suggests that the increase in photocurrent is regulated by the energy barrier associated with the surface states.

Mott-Schottky plots prepared from C_{bulk} values of EIS spectra, which exhibit slopes that are inversely proportional to the charge carrier densities,[17,19] show a strikingly lower slope for the photolyzed photoanodes relative to those not exposed to light (Figure 3c). The photolysis treatments leading to a higher charge carrier density (1.4×10^{20} cm^{-3} to 1.9×10^{21} cm^{-3}) is corroborated by the diminution in resistance (Figures 3a,b). The flat band potential (E_{fb}) of $BiVO_4$ extracted from the *x*-axis intercept of the Mott-Schottky plots is negatively-shifted by 0.25 V after 20 h of UV exposure. This value corresponds reasonably closely to the cathodic shift of onset potential measured in KPi/H_2O_2 (0.23 V, Figure 2c). (Note that Mott-Schottky plots derived from C_{bulk} values of EIS spectra are known to be positively shifted relative to idealized V_{fb} values.)[17,20] A more negative flat band potential provides a higher quasi-Fermi level of electrons ($E_{F,n}$) that drives a greater separation with the quasi-Fermi level of holes ($E_{F,p}$), that leads to a difference of photovoltage generation (0.24 V, Figure 2b). A qualitative energy level diagram summarizing the potential shifts and photovoltage generation is provided in Figure S7.

The foregoing data suggest that passivation of surface states by UV curing is responsible for the lower onset potentials. We therefore set out to gain structural information of the surface by examining the films by X-ray photoelectron spectroscopy (XPS; Figure 3d). The spectra obtained on the samples before and after curing contained the signature oxygen 1s, vanadium 2p (Figure 3d), and bismuth 4f (Figure S8) signals. While the vanadium and bismuth signals displayed no changes before and after photolysis, the oxygen 1s spectroscopic signals were affected. The oxygen 1s peaks at 530.3 eV and 532.3 eV have been ascribed to lattice oxygen and non-uniform surface sites (such as dangling oxygen), respectively (Figure 3d).[21,22] It has been purported that the peaks at ~532 eV correspond to defect sites (e.g., dangling oxo or hydroxy groups) at the surface.[22–24] These are believed to introduce half-filled energy states in the band gap that result in a trapping of charges on the interface of electrode/electrolyte and a Fermi level pinning effect. This situation leads to a lower charge carrier density (Figure 3c). It also consumes of external bias by the surface states (in addition to the depletion layer),[15,17,20] which is corroborated by the high onset potential in H_2O_2 (Figure 2c). The non-uniform surface sites were confirmed by high-resolution transmission electron microscopy (HRTEM),[25,26] with a higher level of crystallinity being observed on the film after 20 h of photolysis (Figure S9b).

This 532.3 eV-XPS signal was significantly diminished for the photolyzed film (Figure 3d), and the ratio of O and Bi atoms at the surface also decreased significantly after UV radiation (from 6:1 to 4:1; Table S1), offering direct evidence

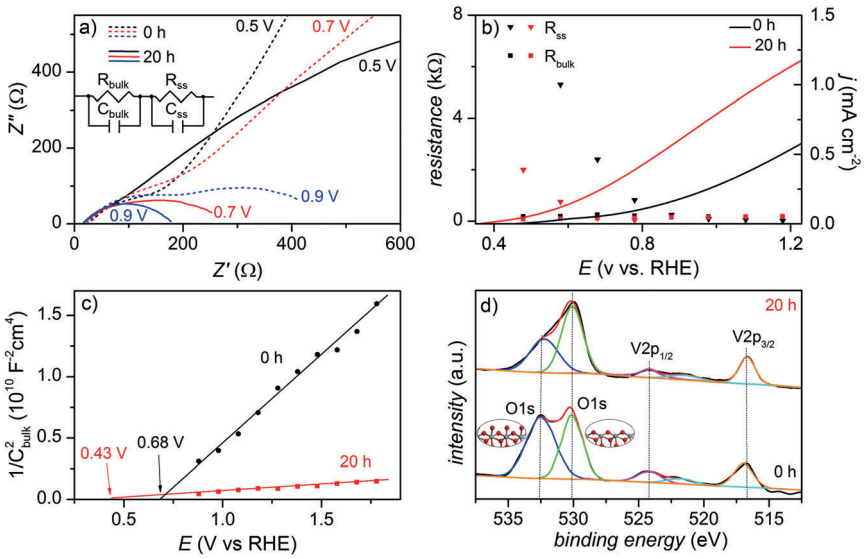

Figure 3. a) Nyquist plots of $BiVO_4$ with 0 h (dashed) and 20 h (solid) UV curing under 0.5 V (black), 0.7 V (red) and 0.9 V (blue) vs. RHE. The first and second semicircles correspond to the bulk (R_{bulk} and C_{bulk}) and surface states (R_{ss} and C_{ss}) shown in the inset image of equivalent circuit model, respectively. b) Resistance–potential plots of the bulk $BiVO_4$ (R_{bulk}, triangles) and surface states (R_{ss}, circles) with 0 h (black) and 20 h (red) UV curing, and the current densities–potential curve of PEC water oxidation. c) Mott–Schottky plots of $BiVO_4$ with 0 h (black) and 20 h (red) UV curing. The intercepts on *X*-axis represent the flat band potentials and the slopes are inversely proportional to the charge carrier densities. d) O 1s and V 2p peaks of $BiVO_4$ with 0 h (black) and 20 h (red) UV curing in XPS spectra normalized to V $2p_{3/2}$ signal. The inset images represent the possible structures of crystalline oxygen (530.3 eV) and oxygen-based defect sites (532.3 eV) on the surface. The red spheres represent O atoms and gray spheres represent V atoms.

that UV light has induced a process that drives the reduction in the number of oxygen atoms. This atomic rearrangement not only releases the charges trapped in the surface states, and thusly a higher charge carrier density in Mott–Schottky plots (Figure 3c), but also minimizes potential loss at the surface to require a relatively lower bias to drive water oxidation.

This work shows that UV curing of the $BiVO_4$ photoanode leads to a marked improvement in OER PEC properties. The exposure to UV radiation is found to diminish the number of defect sites at the surface (possibly dangling oxygen centers) that are purported to be deleterious to PEC performance. This structural arrangement is corroborated by SEM images that show distinctive morphologies before and after photolysis that reflect surface chemistry. An important outcome of this study is that UV photolysis of bare $BiVO_4$ yields a cathodic shift in onset potential and corresponding photocurrent enhancement that is comparable to the effect of coating photoanodes with cocatalysts. This finding may prove useful in resolving the mechanism of action for composite electrodes in photoelectrocatalysis schemes.

Experimental Section

Photoanodes of $BiVO_4$ were prepared according to a previously documented metal-organic decomposition method.[7] Bismuth nitrate hexahydrate (0.346 g, 0.713 mmol), vanadyl acetylacetonate (0.176 g 0.663 mmol) and tungsten hexachloride (0.02 g, 0.05 mmol) were added to a 10 mL mixture of acetic acid and acetylacetone (1:8.25 *v*/*v*). The dark green solution was sonicated for 15 min and then spin-coated onto an FTO substrate (TEC 15, Hartford Glass Co.) at 1000 rpm for 30 s. Each of the successive 16 coats was annealed at 500 °C for 10 min, with an 8 h annealing step at 500 °C for the last step. The photolysis protocol involved exposing the $BiVO_4$ samples to a UV lamp (Model #: GPH436T5VH, Atlantic Ultraviolet Co.; $\lambda_{max} \sim$ 254 nm and 185 nm; flux = 0.12 mW cm^{-2} at 1 m from lamp, ~10 mW cm^{-2} at 5.5 cm in our experiment) for variable periods of time.

Acknowledgements

Funding from The University of British Columbia 4YF Program, Canada Foundation for Innovation, Canada Research Chairs, and CIFAR is gratefully acknowledged. Dr. Bradford Rose in UBC Bioimaging Facility is gratefully acknowledged for the help of HRTEM imaging.

Keywords: bismuth vanadate · photoelectrocatalysis · solar energy · ultraviolet light · water splitting

[1] M. Grätzel, *Nature* **2001**, *414*, 338 – 344.
[2] N. S. Lewis, D. G. Nocera, *Proc. Natl. Acad. Sci. USA* **2006**, *103*, 15729 – 15735.
[3] M. G. Walter, E. L. Warren, J. R. McKone, S. W. Boettcher, Q. Mi, E. A. Santori, N. S. Lewis, *Chem. Rev.* **2010**, *110*, 6446 – 6473.
[4] Y. Park, K. J. McDonald, K.-S. Choi, *Chem. Soc. Rev.* **2013**, *42*, 2321 – 2337.
[5] T. W. Kim, K.-S. Choi, *Science* **2014**, *343*, 990 – 994.
[6] L. Zhang, E. Reisner, J. J. Baumberg, *Energy Environ. Sci.* **2014**, *7*, 1402.
[7] D. K. Zhong, S. Choi, D. R. Gamelin, *J. Am. Chem. Soc.* **2011**, *133*, 18370 – 18377.
[8] S. K. Pilli, T. E. Furtak, L. D. Brown, T. G. Deutsch, J. A. Turner, A. M. Herring, *Energy Environ. Sci.* **2011**, *4*, 5028.
[9] J. A. Seabold, K.-S. Choi, *J. Am. Chem. Soc.* **2012**, *134*, 2186 – 2192.
[10] M. Zhong, T. Hisatomi, Y. Kuang, J. Zhao, M. Liu, A. Iwase, Q. Jia, H. Nishiyama, T. Minegishi, M. Nakabayashi, et al., *J. Am. Chem. Soc.* **2015**, *137*, 5053 – 5060.
[11] Y. Ma, S. R. Pendlebury, A. Reynal, F. Le Formal, J. R. Durrant, *Chem. Sci.* **2014**, *5*, 2964.
[12] R. Li, H. Han, F. Zhang, D. Wang, C. Li, *Energy Environ. Sci.* **2014**, *7*, 1369.
[13] D. K. Zhong, D. R. Gamelin, *J. Am. Chem. Soc.* **2010**, *132*, 4202 – 4207.
[14] R. D. L. Smith, M. S. Prevot, R. D. Fagan, Z. Zhang, P. A. Sedach, M. K. J. Siu, S. Trudel, C. P. Berlinguette, *Science* **2013**, *340*, 60 – 63.
[15] C. Du, X. Yang, M. T. Mayer, H. Hoyt, J. Xie, G. McMahon, G. Bischoping, D. Wang, *Angew. Chem. Int. Ed.* **2013**, *52*, 12692 – 12695; *Angew. Chem.* **2013**, *125*, 12924 – 12927.
[16] F. Le Formal, N. Tétreault, M. Cornuz, T. Moehl, M. Grätzel, K. Sivula, *Chem. Sci.* **2011**, *2*, 737 – 743.
[17] B. Klahr, S. Gimenez, F. Fabregat-Santiago, J. Bisquert, T. W. Hamann, *J. Am. Chem. Soc.* **2012**, *134*, 16693 – 16700.
[18] B. Iandolo, A. Hellman, *Angew. Chem. Int. Ed.* **2014**, *53*, 13404 – 13408; *Angew. Chem.* **2014**, *126*, 13622 – 13626.
[19] B. Klahr, S. Gimenez, F. Fabregat-Santiago, T. Hamann, J. Bisquert, *J. Am. Chem. Soc.* **2012**, *134*, 4294 – 4302.
[20] B. Klahr, S. Gimenez, F. Fabregat-Santiago, J. Bisquert, T. W. Hamann, *Energy Environ. Sci.* **2012**, *5*, 7626.
[21] S. Rahimnejad, J. H. He, W. Chen, K. Wu, G. Q. Xu, *RSC Adv.* **2014**, *4*, 62423 – 62429.
[22] D. Li, W. Wang, D. Jiang, Y. Zheng, X. Li, *RSC Adv.* **2015**, *5*, 14374 – 14381.
[23] X. Zhang, J. Qin, Y. Xue, P. Yu, B. Zhang, L. Wang, R. Liu, *Sci. Rep.* **2014**, *4*, DOI: 10.1038/srep04596.
[24] M. Huang, Y. Zhang, F. Li, Z. Wang, Alamusi, N. Hu, Z. Wen, Q. Liu, *Sci. Rep.* **2014**, *4*, DOI: 10.1038/srep04518.
[25] G. Xi, J. Ye, *Chem. Commun.* **2010**, *46*, 1893.
[26] X. Shi, I. Y. Choi, K. Zhang, J. Kwon, D. Y. Kim, J. K. Lee, S. H. Oh, J. K. Kim, J. H. Park, *Nat. Commun.* **2014**, *5*, 1 – 8.

Received: October 13, 2015
Revised: November 7, 2015
Published online: ■■ ■■, ■■■■

Communications

Photoelectrocatalysis

T. Li, J. He, B. Peña,
C. P. Berlinguette* ——— ▮▮▮▮–▮▮▮▮

Curing $BiVO_4$ Photoanodes with Ultraviolet Light Enhances Photoelectrocatalysis

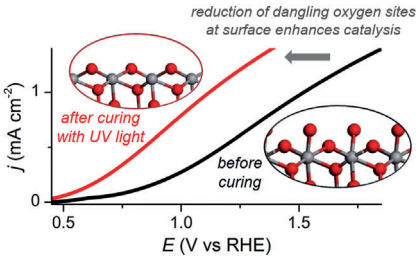

UV curing enhances activity: Exposure of $BiVO_4$ photoanodes to ultraviolet radiation yields a cathodic shift in onset potential and an improvement in photocurrent of water oxidation comparable to the effects of electrocatalysts.